DOI: 10.1002/chem.200801051

Three Polymorphic Forms of the Co-Crystal 4,4′-Bipyridine/Pimelic Acid and their Structural, Thermal, and Spectroscopic Characterization

Dario Braga,*[a] Giuseppe Palladino,[a] Marco Polito,[a] Katia Rubini,[a] Fabrizia Grepioni,*[a] Michele R. Chierotti,[b] and Roberto Gobetto*[b]

Abstract: Three crystal forms of the co-crystal 4,4′-bipy/pimelic acid (bipy: bipyridine), $[NH_4C_5\text{-}C_5H_4N]\cdot[HOOC\text{-}(CH_2)_5COOH]$, have been prepared and their relationship investigated by single-crystal X-ray diffraction, variable-temperature X-ray powder diffraction, differential scanning calorimetry and solid-state NMR spectroscopy. Both X-ray and NMR spectroscopic results indicate that no proton transfer takes place, that is, the three crystal forms are true co-crystals of neutral molecules. Forms I and II both convert into Form III at high temperature, Forms II and III being the thermodynamically stable forms at room and high temperature, respectively.

Keywords: co-crystals · hydrogen bonds · NMR spectroscopy · polymorphism · solid-state structures

Introduction

The investigation of crystal forms, that is, solvates, salts, co-crystals and their respective polymorphs, as well as of amorphous solid phases has become one of the major issues of modern solid-state and materials chemistry.[1] This interest stems from the realization that different crystal forms of the same chemical entity may be exploited in different environments and/or for different scopes depending on the physicochemical characteristics of the compound, and its utilization or processability. Moreover, these features are of great consequence in patenting and marketing issues.[2] Even though crystal polymorphism is well-known and widely studied,[3] the structural, thermodynamic and kinetic factors associated with the nucleation and crystallization of molecular compounds are not yet fully understood. The experimental investigation of crystal polymorphism is still mainly based on a systematic, and sometimes tedious, exploration of all possible crystallization and interconversion conditions[3] ("polymorph screening"), whereas theoretical polymorph prediction is still embryonic.[4]

The screening of different crystal forms of a compound is not only an academic challenge but is also becoming one of the most important goals in the pharmaceutical industry, because the majority of drugs are administered as solids, and solid-state properties significantly influence the bioavailability and stability of the final product. When two or more polymorphs occur, a full characterization of these forms and of the relationship among the different solid phases should be obtained, which is best achieved by using complementary techniques, such as X-ray diffraction and differential scanning calorimetry (DSC) combined with IR, Raman and solid-state NMR (SS NMR) spectroscopy. This also applies to co-crystals, that is, the association in the solid state of different molecules, which have been argued to represent a new route to improved drugs or materials and possibly to be less prone to polymorphism.[1m,n]

We have been involved for some time in the engineering of crystalline materials starting from a knowledge of the supramolecular bonding capacity of the component building blocks. In our studies, as well as in those of many other research groups worldwide, the hydrogen bond has been the interaction of choice.[5] The hydrogen bond allows a certain degree of predictability as far as the structure of the aggregate is concerned, predictability being at the core of any crystal engineering exercise. Together with the use of hydro-

[a] Prof. D. Braga, Dr. G. Palladino, Dr. M. Polito, Dr. K. Rubini, Prof. F. Grepioni
Dipartimento di Chimica "G. Ciamician"
Università degli studi di Bologna
Via Selmi 2, 40126 Bologna (Italy)
Fax: (+39) 0512099456
E-mail: dario.braga@unibo.it
fabrizia.grepioni@unibo.it

[b] Dr. M. R. Chierotti, Prof. R. Gobetto
Dipartimento di Chimica I.F.M. Università di Torino
Via P. Giuria 7, 10125 Torino (Italy)
Fax: (+39) 0116707855
E-mail: roberto.gobetto@unito.it

gen-bonding interactions to assemble (or rather "to let self-assemble") components in the solid state, we have explored direct combination between solid reactants, with or without the presence of small quantities of solvent, to prepare crystalline materials under essentially solvent-free conditions[6]

Herein, we apply some of our previous findings to the preparation and full characterization by powder and single-crystal X-ray diffraction, calorimetric and spectroscopic (^{1}H magic angle spinning (MAS), 2D ^{1}H double-quantum (DQ) MAS, ^{13}C and ^{15}N cross-polarization (CP) MAS NMR) methods of the co-crystalline material obtained by reacting 4,4′-bipyridine (bipy) and pimelic acid. We provide evidence for the existence of three crystal modifications of the 1:1 co-crystal (hereafter termed Forms I, II and III) and the crystallization conditions under which these crystals can be prepared, separated and/or interconverted.

Furthermore, we employ grinding, kneading (also called "wet grinding" or "solvent drop grinding")[7] and vapour digestion[8] methods to obtain these crystal forms besides conventional solution crystallization methods.

Results and Discussion

Forms I–III: How they are obtained and how they transform into each other: Forms I and II of the co-crystal 4,4′-bipy/pimelic acid, $[NH_4C_5\text{-}C_5H_4N]\cdot[HOOC(CH_2)_5COOH]$, were obtained by dissolution in hot water (70 °C) of an equimolar mixture of solid 4,4′-bipy and pimelic acid, previously ground together in an agate mortar. Rapid cooling of the aqueous solution in an ice bath affords single crystals of Form I, which are needle-shaped, whereas slow cooling of the aqueous solution yields prismatic single crystals of Form II, which have a block-like habit. Form II can also be obtained in a kneading experiment, in which the reagents are ground together in the presence of a small drop of THF or MeOH, and in a vapour digestion experiment by grinding together equimolar quantities of 4,4′-bipy and pimelic acid and leaving the polycrystalline powder under an atmosphere of different solvent vapours (MeOH, H_2O or THF; see the Experimental Section). Single crystals of Form III could only be obtained by slow evaporation at 120 °C of a solution obtained by dissolution of an equimolar mixture of reagents in hot dimethyl sulfoxide (DMSO).

The relationship between the three crystal forms was investigated by DSC, powder X-ray diffraction and SS NMR spectroscopy. In all cases, X-ray single-crystal data, besides an exact knowledge of the structure of the products, allowed comparison between the powder diffractograms measured on the reaction products and those calculated on the basis of the single-crystal structures. Details of the various experiments will be provided below. Scheme 1 summarises the relative stability of the three forms and the transformation conditions.

Form II is the thermodynamically most stable form at room temperature. Crystals of Form I left in water convert spontaneously into Form II in a matter of a few days. Polycrystalline Form III can easily be obtained by heating crystals of Form II: the process can be followed both by variable-temperature X-ray powder diffraction and DSC. Crystals of Form III, once formed, can be cooled down to room temperature, where they remain as a metastable form. Only traces of the conversion Form III→Form II are detectable by X-ray powder diffraction if the cooling process is very slow (see below). On the other hand, kneading of Form III with a drop of water affords rapid and complete transformation into Form II. Both Form I and Form II can readily be transformed into Form III by overnight heating at 120 °C in an oven.

DSC measurements allowed analysis of the monotropic/enantiotropic nature of the polymorphic systems. As can be seen in Figure 1, the conversion of Form I into Form III (T = 92.3 °C, onset) is an endothermic process, and therefore Forms I and III are enantiotropically related. Melting of Form III is observed at 141.1 °C (onset).

Figure 2 shows the thermal behaviour of Form II on heating. Conversion into Form III (T = 102.9 °C, onset) is observed at a higher temperature with respect to Form I. The process is endothermic; therefore, Forms II and III also constitute an enantiotropic system. The two broad and shallow peaks on the right and left side of the Form II→Form III transition point are due to traces of unreacted pimelic acid (which first undergoes a phase transition and then melts),

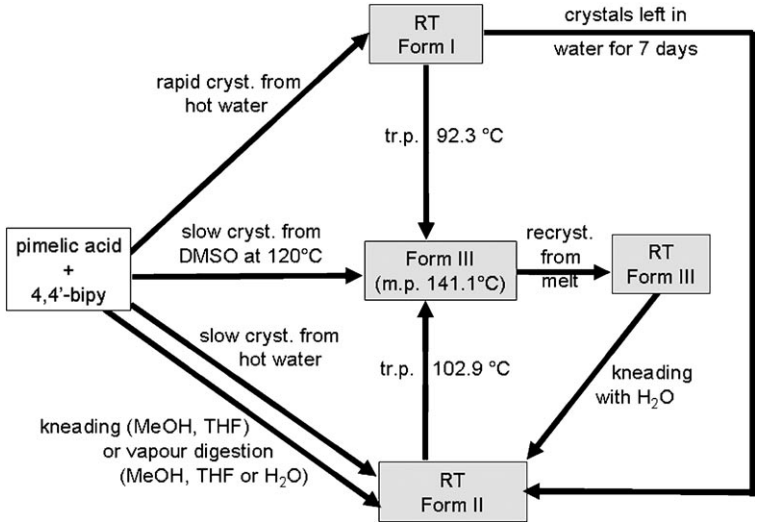

Scheme 1. Preparation and transformation conditions of the three crystal forms of 4,4′-bipy/pimelic acid (tr.p.: transition point; m.p.: melting point).

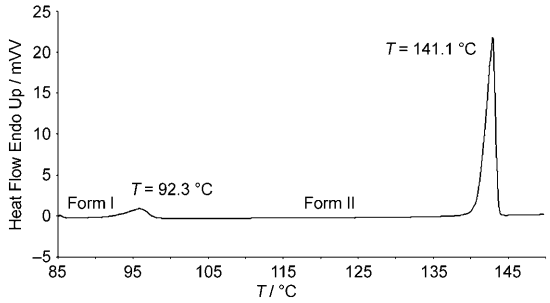

Figure 1. DSC trace of Form I.

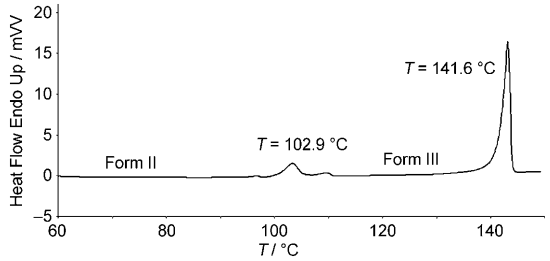

Figure 2. DSC trace of Form II (peaks before and after the transition point are due to traces of unreacted pimelic acid).

not revealed by X-ray diffraction. Their nature was confirmed by intentional addition of a known quantity of pimelic acid to a Form II sample and subsequent observation of an increase in the enthalpy content of the corresponding peaks.

Figure 3 shows the thermal behaviour of Form III on heating. A single peak corresponding to melting is observed. DSC measurements on cooling after melting of Form III only show one exothermic event corresponding to the crystallization of Form III, and no conversion is observed to Form II. This must certainly be due to kinetic "inertia" of the system, which allows Form III to exist at room temperature as a metastable form.

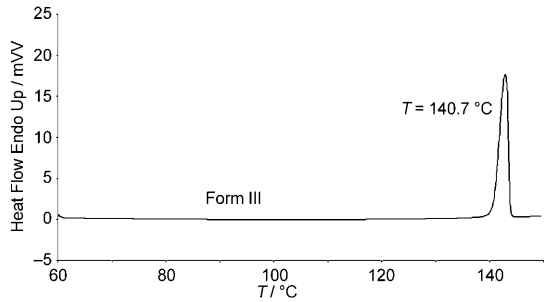

Figure 3. DSC trace of Form III.

On the basis of temperature and ΔH values for the transition and melting processes obtained from the DSC measurements (see the Experimental Section), we can draw a qualitative energy versus temperature diagram,[9] which graphically summarises the thermodynamic relationship of the three forms (see Figure 4). Both Forms I and II transform endothermically to Form III; therefore, according to the "heat of transition rule",[9] the two polymorphs are enantiotropically related to Form III, which is the thermodynamically stable form above the transition temperature. No monotropic transition between Form I and II has been observed, but, because crystals of Form I spontaneously convert into Form II at room temperature in aqueous solution, we can conclude that Form II is the stable form below the II→III transition point. In addition, both the transition temperature and ΔH value for the II→III transition are higher than those observed for the I→III transition, which is also in agreement with the higher stability of Form II at room temperature. Form III has a high kinetic inertia and does not convert back to Form II on cooling.

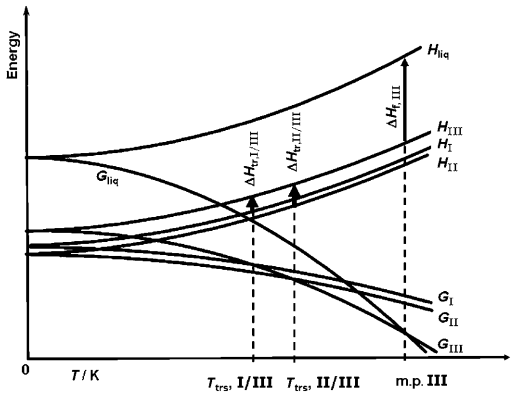

Figure 4. Qualitative energy versus temperature diagram of the three polymorphs. H, enthalpy; G, Gibbs free energy; ΔH_f, heat of fusion; ΔH_{tr}, heat of transition; liq, liquid phase (melt); T_{tr}, transition temperature. Thermal data from DSC.

Structural characterization of Forms I–III: Interestingly, it has also been possible to structurally characterise all three forms by single-crystal X-ray diffraction. Form I crystallises with a rod-like habit, Form II shows a block-like habit (as shown by the photographs in Figure 5), whereas crystals of Form III have a more irregular shape and are inhomogeneous in sise.

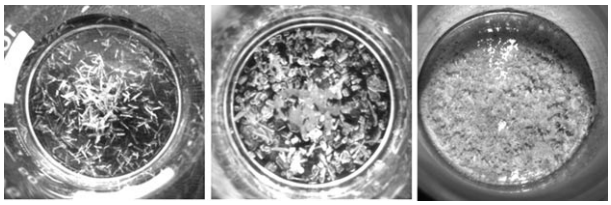

Figure 5. From left to right: crystals of Forms I–III, as obtained from solution.

The structural characterization (see Experimental Section) allowed a comparison of the three crystal forms in

detail. Figure 6 shows that the main packing motif is the same in the three crystals, and is represented by a wavy chain constituted by an alternate sequence of 4,4′-bipy and

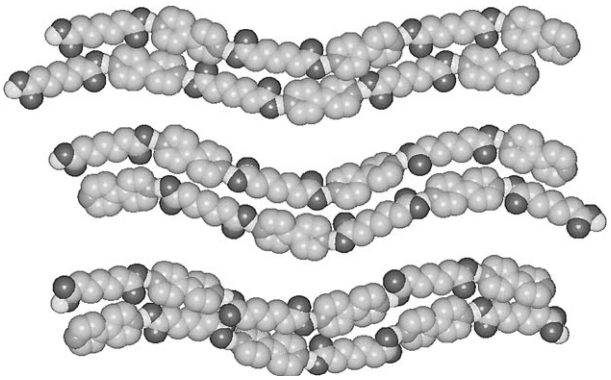

Figure 6. Comparative view of the main packing motifs in the three crystal forms of 4,4′-bipy/pimelic acid; from top to bottom: Form I, II and III. Note that all three forms contain wavy chains created by alternation of 4,4′-bipy and pimelic acid molecules linked by O–H···N hydrogen bonds.

pimelic acid molecules linked by O–H···N hydrogen bonds between the hydrogen atoms of the COOH groups and the nitrogen acceptors. The O(H)···N hydrogen-bonding distances in the three polymorphs do not differ considerably, although it can be noted that, both as ranges and as mean values, they become longer on passing from Form I to II and to III (O···N distances in the ranges 2.638(2)–2.677(2), 2.645(2)–2.697(2) and 2.674(3)–2.756(4) Å; mean values 2.660(2), 2.675(2) and 2.715(4) Å for Forms I, II and III, respectively).

The three polymorphs essentially differ in the relative disposition in their solids of these chains: the most visible difference between Forms I and II, for example, is due to the fact that the acid molecules are almost superimposed in Form I, whereas the chains are shifted with respect to each other in Form II, so as to bring the acid molecules in close contact with the bipyridine moieties (see Figure 6, bottom).

Form III can be considered a conformational polymorph, as the $OH_{(COOH)}$ groups are located almost on the opposite sides of the aliphatic chain (torsion angle ca. 120°, see Figure 7).

Figure 8 shows the hydrogen-bonding pattern within the single chains. It can be appreciated that in Form I (Figure 8, top) and in Form II (middle) one in every two N–H···O

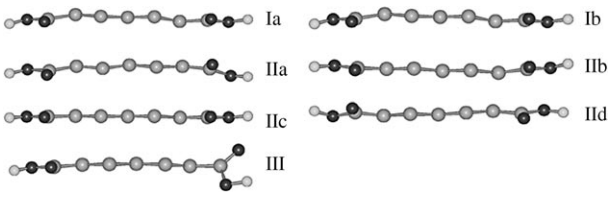

Figure 7. Conformation of the two, four and one independent pimelic acid molecules in crystalline Forms I, II and III, respectively.

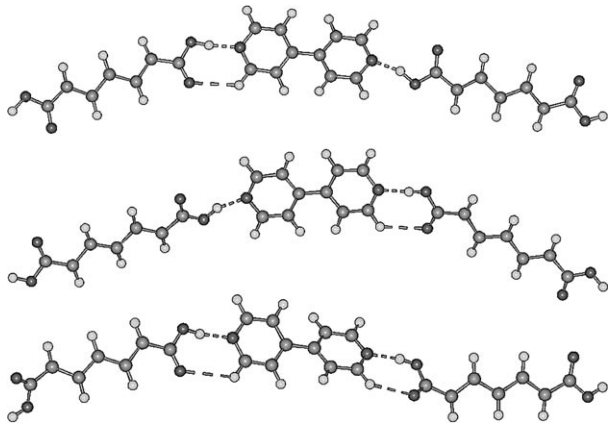

Figure 8. N–H···O and C–H···O hydrogen bonds within the infinite chains in crystalline Form I (top), II (middle) and III (bottom). It can be seen that alternate COOH groups are involved in the creation of dimers in Forms I and II, whereas all COOH groups produce dimers in Form III.

bonds is accompanied by the presence of a short C–H···O interaction (from 2.66 to 2.67 Å in Form I, and from 2.54 to 2.62 Å in Form III), with formation of a hydrogen-bonded dimer. This pattern resembles the one observed years ago for glutaric and adipic acid adducts with 4,4′-bipy.[5g] The pattern changes in Form III, as dimer formation is observed for all carboxylic groups (C–H···O distances of 2.44 and 2.85 Å).

Variable-temperature X-ray diffraction experiments: The phase transformations of the three crystal forms were investigated by variable-temperature X-ray powder diffraction experiments. Samples of 4,4′-bipy/pimelic acid co-crystals of Forms I and II were first obtained from solution, and unambiguously identified as pure polymorphic co-crystals by comparing the X-ray powder diffraction patterns measured at room temperature with those calculated on the basis of the single-crystal structures (see Figure 9).

Forms I and II were heated from 25 to 110 °C, and diffraction patterns were recorded every 5 °C in the range 70–110 °C, each time leaving the sample at the new temperature for 3 min before recording the pattern. Figure 10 shows the diffraction patterns of Forms I and II at 25 and 110 °C. On heating, both forms convert to the same crystal phase, which has been identified as Form III by comparing the diffractograms measured back to room temperature with those calculated on the basis of the single-crystal data (Figure 11). On cooling Form III from 110 °C to room temperature, the kinetic inertia of this form is such that no traces of Form II are detectable at room temperature.

The powder patterns of the 110 °C phase obtained from Forms I and II (Figure 10), however, are different from the one observed for Form III at room temperature. For this reason, Form III was also subjected to the same variable-temperature experiment (see Figure 12a), and its pattern at 110 °C compared with those obtained for Forms I and II: it can be seen that the three patterns are exactly superimposable (see Figure 12b).

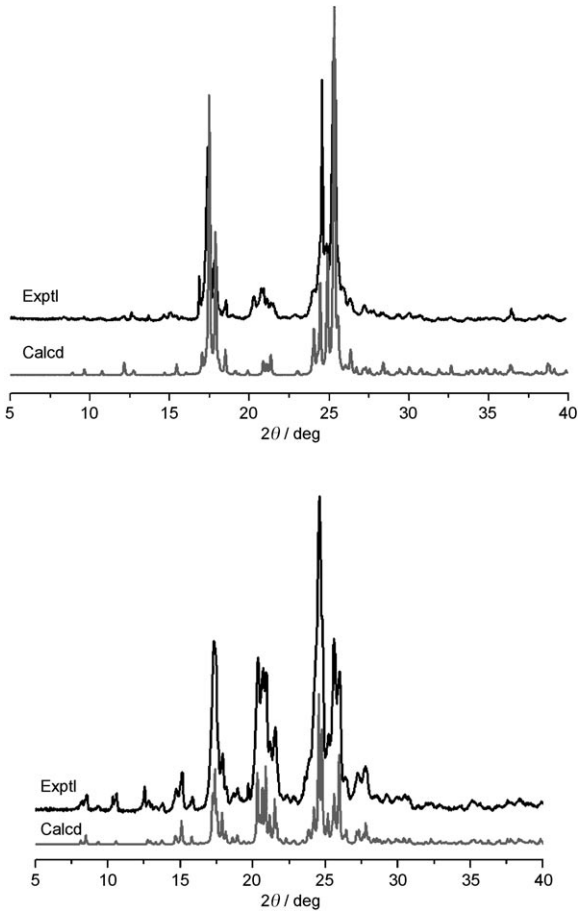

Figure 9. Comparison of the X-ray powder diffraction patterns measured at RT and those calculated on the basis of the single-crystal structures for Form I (top) and II (bottom).

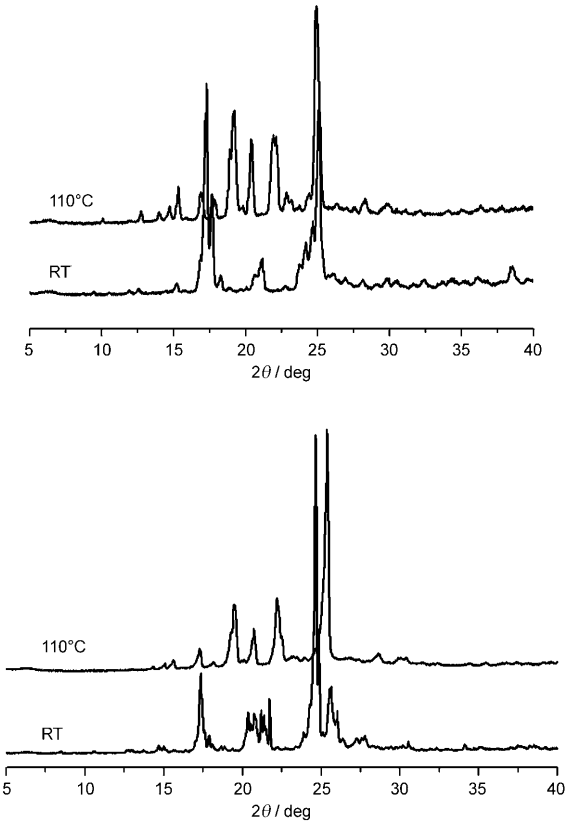

Figure 10. Diffraction patterns measured at RT and 110°C on pure samples of Form I co-crystal (top) and II co-crystal (bottom).

We then heated Form III from 25 to 110°C (and cooled it again to 25°C) and recorded powder patterns every 10°C to observe the change in the pattern profile with temperature. A continuous shift of the peaks can be seen, which is attributed to continuous changes in the cell parameters due to thermal expansion (on heating) or contraction (on cooling). An expanded section of the pattern is shown in Figure 13. The change in the cell parameters, however, is not isotropic (see Figure 14). As a result, patterns of Form III at 25 and 110°C look quite different, but they refer to the same phase (as observed in the DSC measurement).

In addition, we can exclude with confidence the formation of decomposition products at 110°C, because 1) on cooling the sample (that was heated to 110°C) back to room temperature, the room-temperature pattern of Form III is fully restored (Figure 11) and 2) a thermogravimetric analysis (TGA) measurement on Form III shows no weight loss up to 130°C (see Figure 15).

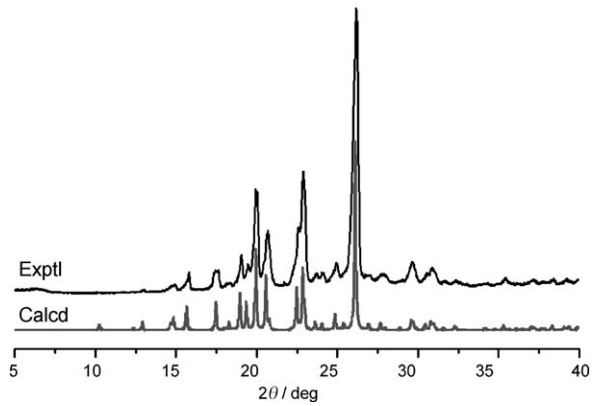

Figure 11. Comparison of the experimental patterns obtained by heating Form II to 110°C and cooling measured back at RT and that calculated on the basis of single-crystal data of Form III.

SS NMR spectroscopic data: It is well-known that SS NMR spectroscopy is a reliable tool for the distinction of different crystalline and amorphous phases and polymorphs.[10] It provides useful information on both the structure and the conversion process between polymorphs.[11] Moreover, because it refers to the short- rather than the long-range order, it can show which site or functional group differs from one form to another or give information on inter- and intramolecular weak interactions.[12] Recently, not only have ^{13}C and ^{15}N nuclei been observed but also, with the development of new probes able to spin the rotor up to 50 kHz, ^{1}H spectra are routinely feasible.[13] This new approach opens innovative perspectives in crystal engineering for the study of hy-

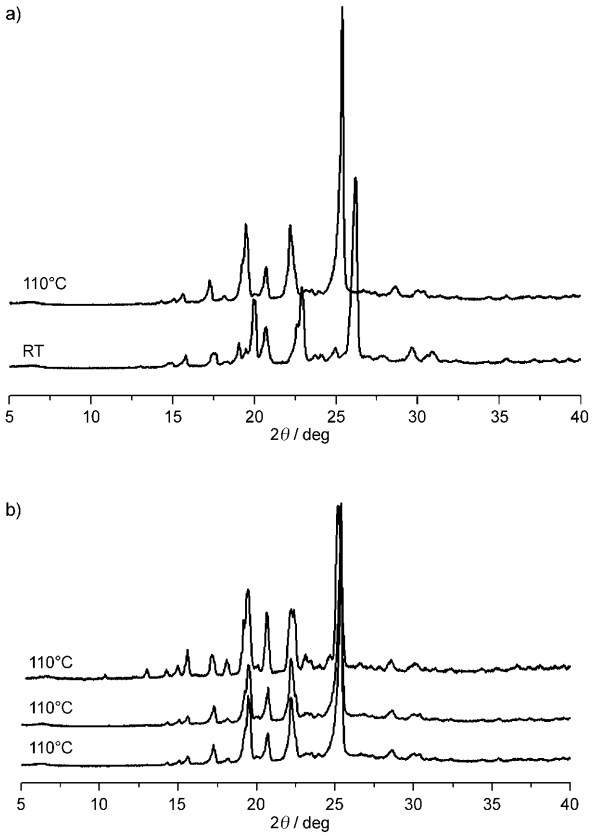

Figure 12. a) Comparison of the diffraction patterns measured at RT and 110 °C on a pure sample of Form III co-crystal. b) Comparison of the diffraction patterns observed for Forms I (top), II (middle) and III (bottom) at 110 °C.

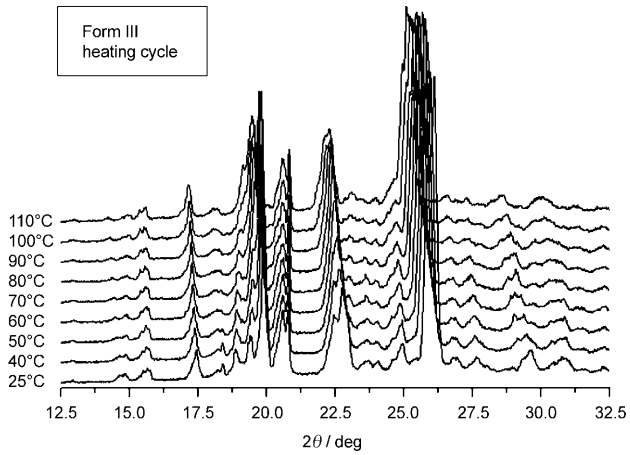

Figure 14. Form III: The whole pattern for the heating process; for sake of clarity, the pattern has been expanded. It can be appreciated how the shift is not always towards lower angles, due to an anisotropic change of the cell parameters.

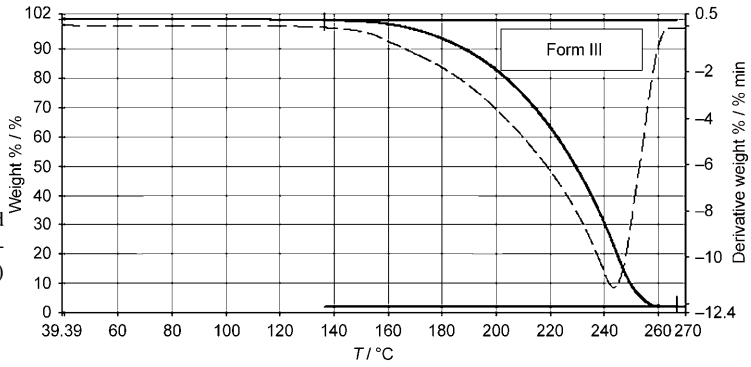

Figure 15. TGA trace of Form III, which shows that the compound is thermally stable up to 130 °C. ——: TGA trace; -----: first derivative.

drogen-bond interactions and in the evaluation of the proton proximity in supramolecular adducts, crystals and polymorphs. 1D ^{1}H spectra can provide valuable information on the hydrogen-bond strength, because the chemical shift parameter is directly correlated to the X−H bond polarization and thus to the energy of the interaction. Schnell et al.[14] have shown that the extension of the experiment to a second dimension, namely 2D ^{1}H DQ MAS, offers new information about, for example, the proximity or connectivity of different nuclei. In ^{1}H–^{1}H DQ NMR spectroscopy, the generation of DQ coherence requires the existence of a dipolar coupling between two protons. Thus, the observation of particular DQ peaks implies the existence of a sufficient dipolar coupling between the respective nuclei. In this way, detailed information about internuclear proximities can be readily obtained from the 2D peaks.

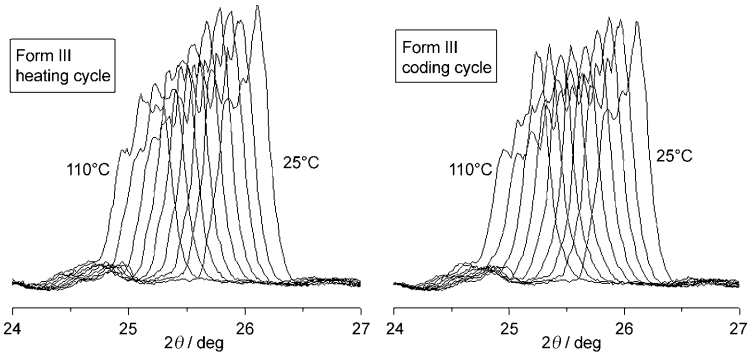

Figure 13. Form III: Expansion of the 24–27° of the 2θ zone, which shows how the peak positions shift continuously on heating from 25 to 110 °C (left) and on cooling back from 110 to 25 °C (right).

Here, we combine the information arising from ^{1}H (1D and 2D), ^{13}C and ^{15}N SS NMR spectroscopic experiments with the aim to a) check spectroscopic differences among polymorphs, b) assess the co-crystal or salt nature of the polymorphs and c) probe hydrogen-atom proximities.

All NMR spectroscopic data with their relative assignments

are listed in Table 1. Due to the very similar crystal packing of the three forms, the ^{13}C CPMAS spectra (Figure 16) present comparable features: the high-frequency region of the spectra is characterised by carboxylic signals around $\delta =$ 175–176 ppm. The bipyridine resonances fall at about $\delta =$ 147 and 123 ppm with the former attributed to quaternary and H*C*–N carbon atoms and the latter related to CH carbon atoms. The CH_2 carbon atoms of the acid moiety give rise to peaks around $\delta = 36$–31 ppm.

Table 1. ^{13}C, ^{15}N and ^{1}H NMR spectroscopic chemical shifts [ppm] with assignments of the three crystal forms (Forms I, II and III) of the 4,4′-bipy/pimelic acid co-crystal.

	Form I	Form II	Form III
^{13}C data			
COOH (acid)	176.2	175.3	175.6
H*C*–N (bipy)	150.1	149.9	150.1
	147.8	147.2	147.3
C_q (bipy)[a]	144.2	146.8	146.9
		144.7 sh	
CH (bipy)	124.4	123.0	123.2
	122.9	121.6	
	120.6		
CH_2 (acid)	36.6 (α)	35.0 (α)	35.2 (α)
	35.4 (α)	26.0 (β)	26.1 (β)
	25.8 (β)	31.1 (γ)	31.2 (γ)
	31.0 (γ)		
^{15}N data			
N (bipy)	261.5	262.8	263.2
^{1}H data			
proton A (O–*H*···N)	14.32	14.21	14.68
proton B (C*H*)	7.92	7.77	8.31
proton C (CH_2)	1.04	1.05	1.28

[a] Determined by ^{13}C non-quaternary-suppression (NQS) NMR experiments.

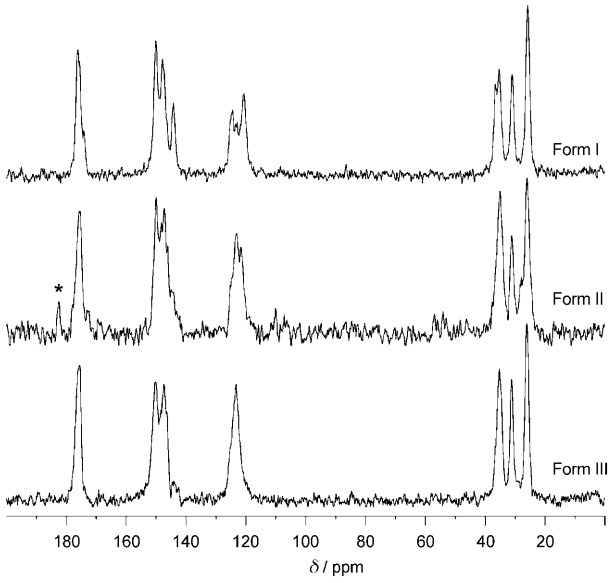

Figure 16. ^{13}C CPMAS spectra of {[NH_4C_5-C_5H_4N]·[HOOC-$(CH_2)_5$COOH]}, Forms I, II and III, recorded at 100.63 MHz with a spinning speed of 12 kHz (the peak marked with * is due to unreacted pimelic acid.)

Small but significant differences among spectra allow the distinction of the three forms, and are in agreement with the same wavy-chain motifs of alternating 4,4′-bipy and pimelic acid molecules linked through O–H···N hydrogen bonds displayed by the three polymorphs.

Another difference concerns the splitting, observed in Form I, of the signal relative to the α-CH_2 group ($\delta = 36.6$ and 35.4 ppm), even though the main difference can be found on the bipyridine moiety. Indeed, Form I shows three CH peaks ($\delta = 124.4$, 122.9 and 120.6 ppm) instead of the two ($\delta = 123.0$ and 121.6 ppm) and one ($\delta = 123.2$ ppm) observed in Forms II and III, respectively. Similar remarks can also be made for the multiplet arising from the overlapping of quaternary and H*C*–N carbon resonances (see Table 1).

To ascertain whether the proton transfer from the acid to the base takes place along the hydrogen bond or, in other words, to determine the co-crystal or salt nature of the polymorph, it is well-known that the ^{13}C chemical shift of the carboxylic carbon atom represents a good indicator of the protonation state of the COOH group.[15a,b] For these compounds, the observed chemical shift (around $\delta = 175$ ppm) is reminiscent of the value previously found for similar adducts containing 1,4-diazabicyclo[2.2.2]octane instead of bipyridine.[15c] In that study, the obtained value was referred to a COOH rather than a COO^- group. This is in agreement with the co-crystal nature of the adducts observed by single-crystal X-ray diffraction and confirmed by ^{15}N CPMAS spectra. Several ^{15}N NMR studies on hydrogen-bonded systems have shown that formation of hydrogen bonds results in high- or low-frequency shifts of the nitrogen signal, according to the type of nitrogen atom and the nature of the interaction.[13c,15d–f] In our case, the free bipyridine nitrogen signal falls at $\delta = 288.2$ ppm, whereas in the three co-crystal forms it falls around $\delta = 262$ ppm. Similar shifts have already been reported by us[16a] and by Limbach and co-workers[16b] for hydrogen-bonded pyridine nitrogen atoms: in the former case for co-crystals between dipyridineferrocene [$Fe(\eta^5$-C_5H_4-$C_5H_4N)_2$] and pimelic acid and in the latter case for pyridine molecules adsorbed on mesoporous silica. Thus, the shift is consistent with a nitrogen atom involved in an O–H···N interaction rather than a charge-assisted $^-$O···H-N^+ hydrogen bond.

The ^{1}H MAS spectra of the three polymorphs (Figure 17) appear quite similar even for the hydrogen-bonded proton signals, which suggests that the higher thermodynamic stability at room temperature of Form II with respect to Forms I and III does not arise from stronger or weaker hydrogen-bond interactions. As mentioned above, the extension to a second dimension of the ^{1}H spectra may provide further information about proton connectivity, proximity and thus about structural differences among the polymorphs.[14a,17]

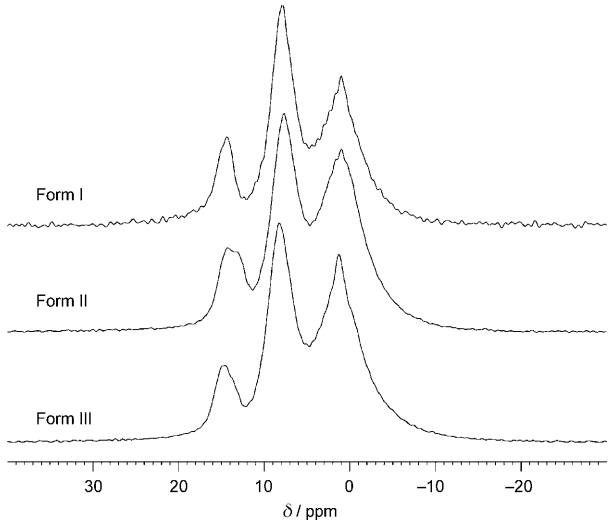

Figure 17. ^{1}H MAS spectra of {[NH_4C_5-C_5H_4N]·[$HOOC(CH_2)_5COOH$]}, Forms I, II and III, recorded at 600.23 MHz with a spinning speed of 32 kHz.

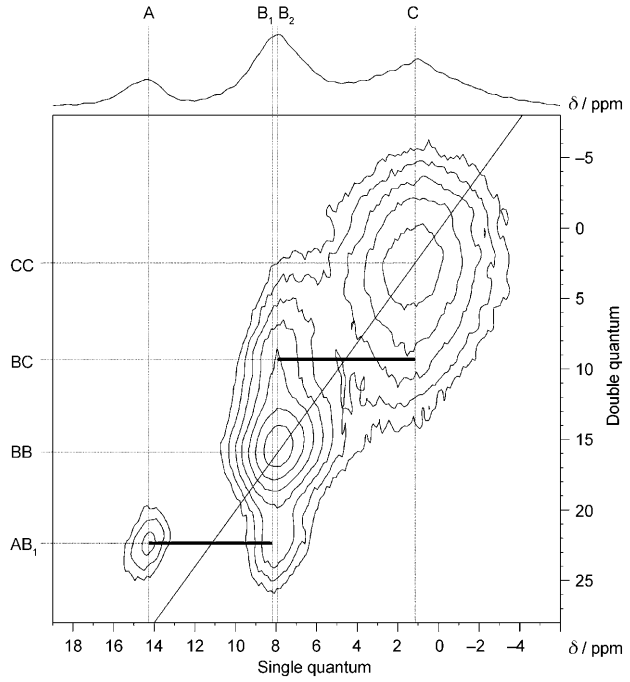

Figure 18. 2D ^{1}H DQ MAS spectrum of {[NH_4C_5-C_5H_4N]·[$HOOC(CH_2)_5COOH$]}, Form I, together with the single-quantum projection.

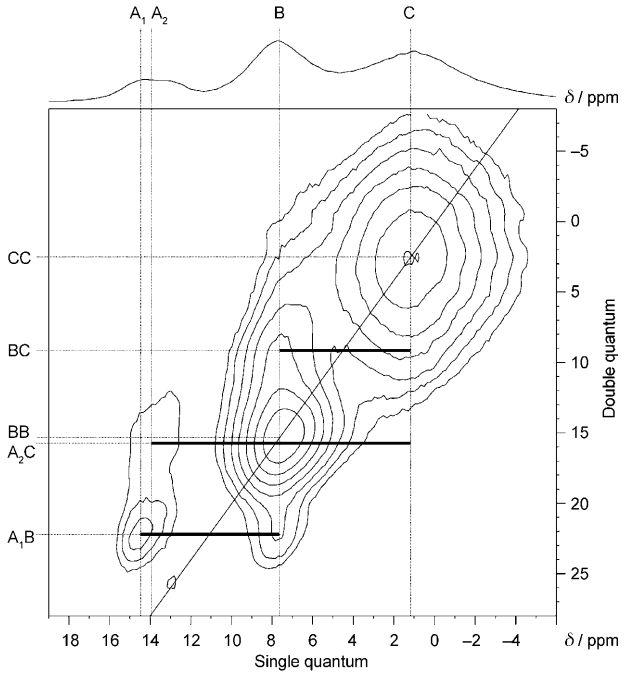

Figure 19. 2D ^{1}H DQ MAS spectrum of {[NH_4C_5-C_5H_4N]·[$HOOC(CH_2)_5COOH$]}, Form II, together with the single-quantum projection.

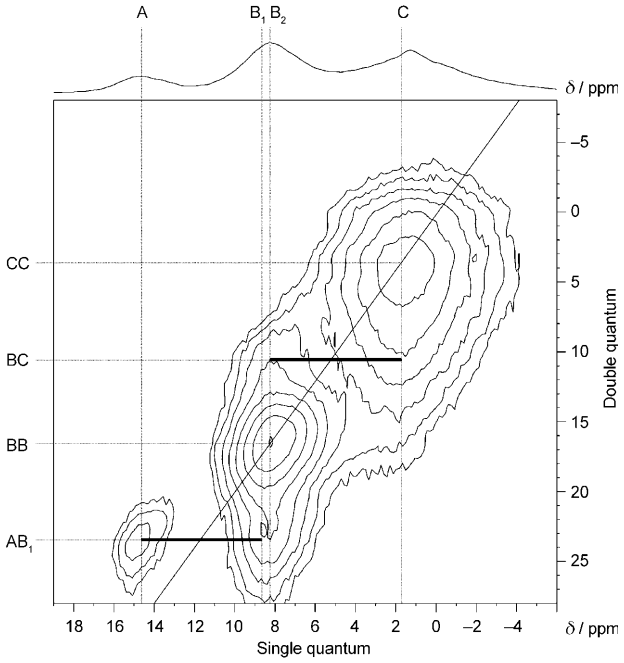

Figure 20. 2D ^{1}H DQ MAS spectrum of {[NH_4C_5-C_5H_4N]·[$HOOC(CH_2)_5COOH$]}, Form III, together with the single-quantum projection.

In the 1D ^{1}H spectra, only three peaks can be distinguished, which correspond to the O−H···N (A), the aromatic protons (B) and the alkyl protons (C) at about $\delta = 14$–15, 7–8 and 1–3 ppm, respectively (Figure 17). The 2D ^{1}H DQ MAS spectra of Forms I–III are reported in Figures 18, 19 and 20, respectively. They show trivial aromatic (BB) and alkyl (CC) auto-peaks and, more interestingly, a BC cross-peak in agreement with the presence of parallel chains running near each other and characterizing the crystal structures. Indeed, by looking at the single-crystal data (see above), in all three polymorphs the crystal packing leads the bipyridine moiety near to an acid molecule of the next chain. Due to the r^{-6} dependence of the dipolar interaction we can say that the observation of the peak above is indicative of a proton–proton distance in the narrow range of about 0.18 to 0.30 nm; this is without recourse to a full quantitative inves-

tigation.[14a] The O–H···N protons (A) give rise to a cross-peak to the *meta*-CH aromatic protons (AB_1 for Forms I and III and A_1B for Form II). In addition to this, in Form II there is some evidence of a weaker cross-peak to the aliphatic protons (A_1C).

Conclusion

We have reported the identification of three polymorphs of a molecular co-crystal formed by the dicarboxylic acid pimelic acid and the 4,4′-bipy molecule. The three polymorphs have been fully characterised by single-crystal and powder X-ray diffraction, calorimetry and ^{1}H MAS (1D and 2D) and ^{13}C and ^{15}N CPMAS NMR spectroscopic experiments. By ^{1}H MAS NMR spectroscopic experiments it has been possible to ascertain that the higher stability of Form II with respect to Forms I and III depends on the crystal packing rather than different hydrogen-bond strengths. Furthermore, the 2D ^{1}H DQ MAS experiments provide reliable information concerning proton proximities, that is, useful for discriminating different crystal packings and hydrogen-bond frameworks.

We have also provided further examples of the possibility of preparing co-crystals by kneading (also called "wet or solvent-drop grinding") and by vapour digestion.[7,8]

Moreover, by combining X-ray data with ^{13}C carboxylic carbon and ^{15}N pyridine nitrogen chemical shifts we were able to conclude that no proton transfer took place from the acid to the base, along the hydrogen bond, in all three crystal forms. In the co-crystal of pimelic acid with $[Fe(\eta^5\text{-}C_5H_4\text{-}C_5H_4N)_2]$,[16a] on the contrary, two different situations were observed depending on the stoichiometry of the adduct: the 1:1 co-crystal is a neutral molecular complex, whereas in the 1:2 co-crystal protonation of the organometallic base takes place. Further studies are also in progress to fully appreciate the factors controlling the positions of hydrogen atoms in acid/base co-crystals. The relationship between molecular salts and co-crystals in multicomponent crystals has been recently discussed.[18]

With respect to the issue that co-crystalline materials might be less prone to polymorphism,[1m,n] we think that this is not so, at least not in co-crystals containing strong hydrogen-bonded units, or synthons. When the hydrogen bonding has been "taken care of", the resulting unit packs in the solid as a van der Waals object, even if, as in this paper, the object is an infinite chain. Small adjustments in the torsional angle of the constituent molecules and/or chains may suffice to produce a new crystalline phase. On the contrary, we think that co-crystals might be less prone to the formation of solvates, as the hydrogen-bonding requirements of one constituent molecule are usually fulfilled by the association with the second molecular entity. We are currently exploring this idea within molecular hydrogen-bonded co-crystals.

Experimental Section

Solid-state and solution syntheses: All reactants were purchased from Aldrich and used without further purification. Reagent-grade solvents and doubly distilled water were used. In all cases, correspondence between the structure of the solid residue and that obtained by single-crystal X-ray diffraction was ascertained by comparing measured X-ray powder diffractograms with those calculated on the basis of single-crystal data.

Solid-state synthesis of Forms II and III of the co-crystal 4,4′-bipy/pimelic acid: The polymorphic modification Form II was prepared by solid-state synthesis. When equimolar quantities of 4,4′-bipy and pimelic acid were manually ground in an agate mortar in the presence of drops of solvent (MeOH, THF), Form II was obtained. Both Forms I and II, placed in an oven at 120 °C, quantitatively transformed into Form III overnight.

Vapour digestion experiments: Form II was also obtained in a vapour digestion experiment by grinding together equimolar quantities of 4,4′-bipy and pimelic acid and leaving the polycrystalline powder under different solvent vapours (MeOH, CH_2Cl_2 and THF). When MeOH or CH_2Cl_2 were used, Form II started to appear after 60 min of exposure, and the transformation was complete after a total exposure time of 90 min. When THF was used, the reaction was complete only after an exposure time of 24 h.

Solution synthesis of Forms I–III of the co-crystal 4,4′-bipy/pimelic acid: Single crystals of Forms I and II suitable for single-crystal X-ray diffraction were obtained by dissolution of a ground equimolar mixture of 4,4′-bipy (0.666 mg, 4.264 mmol) and pimelic acid ($HOOC(CH_2)_5COOH$; 0.683 g, 4.264 mmol) in boiling water. If the solution was cooled quickly in an ice bath, colourless needles of Form I were obtained, whereas slow cooling of the solution yielded colourless prismatic single crystals of Form II.

Single crystals of Form III suitable for X-ray diffraction were obtained by dissolution of a ground equimolar mixture of 4,4′-bipy (0.234 mg, 1.495 mmol) and pimelic acid ($HOOC(CH_2)_5COOH$; 0.240 g, 1.497 mmol) in DMSO at 120 °C. The solution was allowed to evaporate slowly at 120 °C in an oil bath, to yield colourless crystals of Form III.

Calorimetric analysis: Calorimetric measurements were performed with a Perkin–Elmer Pyris Diamond DSC differential scanning calorimeter equipped with a model ULSP 90 intra-cooler. The instrument was calibrated with high-purity standards (indium and cyclohexane) at 5 K min^{-1}. The samples (2–4 mg) were placed in closed aluminium pans. Heating was carried out at 5 °C min^{-1} in the temperature range 60 to 150 °C. Melting point (onset) and enthalpy of fusion for Form III: (141.1 ± 1.0) °C and (46.8 ± 0.5) kJ mol^{-1}, respectively; transition temperature (onset) and enthalpy of transition for Forms I and II: (92.3 ± 0.3) °C, (5.5 ± 0.5) kJ mol^{-1} and (102.9 ± 0.3) °C, (6.7 ± 0.5) kJ mol^{-1}, respectively.

TGA was performed with a Perkin–Elmer TGA-7 apparatus. Heating was carried out in a nitrogen flow (20 cm^3 min^{-1}) and by using a platinum crucible at the rate of 5 °C min^{-1} up to decomposition. The sample weights were in the range 5–10 mg.

Crystal structure determination: Crystal data of all compounds were collected at room temperature on a Bruker ApexII CCD diffractometer. Crystal data and details of measurements are summarised in Table 2. Common to all compounds: $Mo_{K\alpha}$ radiation, $\lambda = 0.71073$ Å, monochromator graphite, $T = 293$ K. SHELX97[19a] was used for structure solution and refinement based on F^2. All non-hydrogen atoms were refined anisotropically. Hydrogen atoms bound to carbon atoms were added in calculated positions and refined riding on their respective carbon atoms. Hydrogen atoms bound to oxygen atoms were all found and refined, with the exception of one of the two hydrogen atoms in Form III, which was found but not refined. SCHAKAL99[19b] was used for the graphical representation of the results. The program PLATON[19c] was used to calculate the hydrogen-bonding interactions. CCDC-678762 (Form I), 678763 (Form II) and 678764 (Form III) contain the supplementary crystallographic data for this paper. These data can be obtained free of charge from The Cambridge Crystallographic Data Centre via www.ccdc.cam.ac.uk/data_request/cif.

Table 2. Crystal data and details of measurements for Forms I–III.

Compound	Form I	Form II	Form III
formula	$C_{17}H_{20}N_2O_4$	$C_{17}H_{20}N_2O_4$	$C_{17}H_{20}N_2O_4$
M_r	316.35	316.35	316.35
system	monoclinic	monoclinic	monoclinic
space group	$P2_1/c$	$P2_1/c$	$P2_1/c$
a [Å]	10.692(1)	42.106(2)	7.9199(7)
b [Å]	41.635(4)	7.3632(3)	9.3588(9)
c [Å]	7.7411(8)	21.7542(9)	22.404(2)
α [°]	90.00	90.00	90.00.
β [°]	107.051(2)	103.002(1)	97.690(1)
γ [°]	90.00	90.00	90.00.
V [Å^3]	3294.5(6)	6571.6(5)	1645.7(3)
Z	8	16	4
ρ_{calcd}	1.276	1.279	1.277
$F(000)$	1344	2688	672
$\mu(Mo_{K\alpha})$ [mm^{-1}]	0.092	0.092	0.092
θ_{max} [°]	28	28	27.5
measured reflns	27394	53462	12657
unique reflns	7430	14900	3523
refined parameters	432	860	212
GOF on F^2	1.042	0.907	0.976
$R1$ [on F, $I>2\sigma(I)$]	0.0474	0.0482	0.0693
$wR2$(on F^2, all data)	0.1140	0.1217	0.2149

Powder diffraction measurements: The identity of the bulk material obtained by either the solid-state or the solution processes and the structures obtained by single crystals was always verified by comparison of calculated and observed powder diffraction patterns. X-ray powder diffractograms were collected on a Panalytical X'Pert PRO automated diffractometer with $Cu_{K\alpha}$ radiation and an X'Celerator detector equipped with an Anton Paar TTK 450 low-temperature camera. The program PowderCell 2.2[19d] was used for calculation of X-ray powder patterns on the basis of the single-crystal structure determinations.

SS NMR spectroscopic measurements: All spectra were recorded on a Bruker Avance II 400 spectrometer operating at 400.23, 100.65 and 40.55 MHz for ^{1}H, ^{13}C and ^{15}N, respectively. ^{13}C and ^{15}N spectra were recorded at room temperature at the spinning speed of 12 kHz. Cylindrical 4-mm-outer-diameter zirconia rotors were employed with a sample volume of 120 mL. A ramp CP pulse sequence was used with a contact time of 3 (^{13}C) or 4 ms (^{15}N), a ^{1}H 90° pulse of 3.35 μs, recycle delays of 15–90 s and about 128 and 3000 transients for the ^{13}C and ^{15}N CPMAS spectra, respectively. A two-pulse phase-modulation decoupling scheme was used with a radio-frequency field of 75 kHz. For the ^{13}C NQS NMR experiments, a dephasing delay of 40 μs was used with a 180° refocusing pulse on the ^{13}C channel of 4.7 μs.

1D and 2D ^{1}H DQ MAS experiments were performed on a 2.5 mm Bruker probe at the spinning speed of 32 kHz. The ^{1}H MAS spectra were acquired with the DEPTH sequence (π/2–π–π) for suppressing the probe background signal. The back-to-back (BABA) recoupling pulse sequence,[20] which efficiently generates DQ coherences in the presence of very fast MAS, was used to acquire 2D ^{1}H DQ MAS NMR spectra with excitation times of one rotor period. For all samples, the ^{1}H 90° pulse length was 3.25 μs, and a recycle delay of 7 s was used. For each of 64 increments of t_1, 128 transients were averaged.

Acknowledgement

We acknowledge financial support from the University of Bologna (postdoctoral fellowship to G.P.) and from MIUR (PRIN2006).

[1] a) B. R. Sreekanth, P. Vishweshwar, K. Vyas, *Chem. Commun.* **2007**, 2375; b) A. D. Bond, *CrystEngComm* **2007**, *9*, 833; c) M. Rafilovich, J. Bernstein, M. B. Hickey, M. Tauber, *Cryst. Growth Des.* **2007**, *7*, 1777; d) G. G. Z. Zhang, R. F. Henry, T. B. Borchardt, X. Lou, *J. Pharm. Sci.* **2007**, *96*, 990; e) A. Jayasankar, D. J. Good, N. Rodríguez-Hornedo, *Mol. Pharm.* **2007**, *4*, 360; f) W. W. Porter III, S. C. Elie, A. J. Matzger, *Cryst. Growth Des.* **2008**, *8*, 14; g) M. T. Kirchner, D. Das, R. Boese, *Cryst. Growth Des.* **2008**, *8*, 763; h) A. V. Trask, W. D. S. Motherwell, W. Jones, *Cryst. Growth Des.* **2005**, *5*, 1013; i) A. V. Trask, W. D. S. Motherwell, W. Jones, *Int. J. Pharm.* **2006**, *114*, 320; j) A. M. Chen, M. E. Ellison, A. Peresypkin, R. M. Wenslow, N. Variankaval, C. G. Savarin, T. K. Natishan, D. J. Mathre, P. G. Dormer, D. H. Euler, R. G. Ball, Z. Ye, Y. Wang, I. Santos, *Chem. Commun.* **2007**, 419; k) D.-K. Bučar, R. F. Henry, X. Lou, T. B. Borchardt, G. G. Z. Zhang, *Chem. Commun.* **2007**, 525; l) S. L. Childs, K. I. Hardcastle, *CrystEngComm* **2007**, *9*, 364; m) Ö. Almarsson, M. J. Zaworotko, *Chem. Commun.* **2004**, 1889; n) P. Vishweshwar, J. A. McMahon, J. A. Bis, M. J. Zaworotko, *J. Pharm. Sci.* **2006**, *95*, 499.

[2] a) W. Cabri, P. Ghetti, G. Pozzi, M. Alpegiani, *Org. Process Res. Dev.* **2007**, *11*, 64; b) F. Lara-Ocha, G. Espinosa-Pérez, *Cryst. Growth Des.* **2007**, *7*, 1213.

[3] a) J. Bernstein, *Polymorphism in Molecular Crystals*, Oxford University Press, Oxford, **2002**, p. 352; b) H. G. Brittain, *Polymorphism in Pharmaceutical Solids*, Marcel Dekker, New York, **1999**, p. 427; c) R. Hilfiker, *Polymorphism*, Wiley-VCH, Weinheim, **2006**.

[4] a) G. M. Day, W. D. S. Motherwell, H. L. Ammon, S. X. M. Boerrigter, R. G. Della Valle, E. Venuti, A. Dzyabchenko, J. D. Dunitz, B. Schweizer, B. P. van Eijck, P. Erk, J. C. Facelli, V. E. Bazterra, M. B. Ferraro, D. W. M. Hofmann, F. J. J. Leusen, C. Liang, C. C. Pantelides, P. G. Karamertzanis, S. L. Price, T. C. Lewis, H. Nowell, A. Torrisi, H. A. Scheraga, Y. A. Arnautova, M. U. Schmidt, P. Verwer, *Acta Crystallogr. Sect. B* **2005**, *61*, 511; b) S. A. Barnett, A. Johnston, A. J. Florence, S. L. Price, D. A. Tocher, *Cryst. Growth Des.* **2008**, *8*, 24.

[5] a) C. B. Aakeröy, I. Hussain, S. Forbes, J. Desper, *CrystEngComm* **2007**, *9*, 46; b) C. B. Aakeröy, J. Desper, M. E. Fasulo, *CrystEngComm* **2006**, *8*, 586; c) D. Braga, L. Maini, M. Polito, F. Grepioni, *Struct. Bonding* **2004**, *111*, 1; d) C. C. Wilson, *Acta Crystallogr. Sect. B* **2001**, *57*, 435; e) T. Steiner, I. Majerz, C. Wilson, *Angew. Chem.* **2001**, *113*, 2728; *Angew. Chem. Int. Ed.* **2001**, *40*, 2651; f) D. Wiechert, D. Mootz, *Angew. Chem.* **1999**, *111*, 2087; *Angew. Chem. Int. Ed.* **1999**, *38*, 1974; g) V. R. Pedireddi, S. Chatterjee, A. Ranganathan, C. N. R. Rao, *Tetrahedron* **1998**, *54*, 9457; h) S. Varaghese, V. R. Pedireddi, *Chem. Eur. J.* **2006**, *12*, 1597.

[6] a) D. Braga, S. L. Giaffreda, F. Grepioni, A. Pettersen, L. Maini, M. Curzi, M. Polito, *Dalton Trans.* **2006**, 1249; b) D. Braga, L. Maini, S. L. Giaffreda, F. Grepioni, M. R. Chierotti, R. Gobetto, *Chem. Eur. J.* **2004**, *10*, 3261; c) D. Braga, L. Maini, M. Polito, L. Mirolo, F. Grepioni, *Chem. Eur. J.* **2003**, *9*, 4362; d) D. Braga, M. Curzi, F. Grepioni, M. Polito, *Chem. Commun.* **2005**, 2915; e) D. Braga, M. Curzi, M. Lusi, F. Grepioni, *CrystEngComm* **2005**, *7*, 276; f) A. Pichon, A. Lazuen-Garay, S. L. James, *CrystEngComm* **2006**, *8*, 211; g) A. V. Trask, D. A. Haynes, W. D. S. Motherwell, W. Jones, *Chem. Commun.* **2006**, 51.

[7] a) A. V. Trask, W. D. S. Motherwell, W. Jones, *Cryst. Growth Des.* **2005**, *5*, 1013; b) A. V. Trask, W. D. S. Motherwell, W. Jones, *Int. J. Pharm.* **2006**, *114*, 320; c) A. M. Chen, M. E. Ellison, A. Peresypkin, R. M. Wenslow, N. Variankaval, C. G. Savarin, T. K. Natishan, D. J. Mathre, P. G. Dormer, D. H. Euler, R. G. Ball, Z. Ye, Y. Wang, I. Santos, *Chem. Commun.* **2007**, 419; d) D.-K. Bučar, R. F. Henry, X. Lou, T. B. Borchardt, G. G. Z. Zhang, *Chem. Commun.* **2007**, 525; e) S. L. Childs, K. I. Hardcastle, *CrystEngComm* **2007**, *9*, 364; f) B. R. Sreekanth, P. Vishweshwar, K. Vyas, *Chem. Commun.* **2007**, 2375; g) D. Braga, L. Maini, *Chem. Commun.* **2004**, 976; h) M. Reutzel, C. G. Choo, *J. Am. Chem. Soc.* **1993**, *115*, 4411; i) W. H. Ojala, M. C. Etter, *J. Am. Chem. Soc.* **1992**, *114*, 10228; j) V. R. Pedireddi, W. Jones, A. P. Chorlton, R. Docherty, *Chem. Commun.* **1996**, 987; k) A. V. Trask, W. D. S. Motherwell, W. Jones, *Chem. Commun.* **2004**, 890; l) A. V. Trask, N. Shan, W. D. S. Motherwell, W. Jones, S. Feng, R. B. H. Tan, K. J. Carpenter, *Chem. Commun.* **2005**, 880.

[8] a) D. Braga, S. L. Giaffreda, K. Rubini, F. Grepioni, M. R. Chierotti, R. Gobetto, *CrystEngComm* **2007**, *9*, 39; b) D. Braga, S. L. Giaffreda, F. Grepioni, *Chem. Commun.* **2006**, 3877; c) N. Shan, F. Toda, W. Jones, *Chem. Commun.* **2002**, 2372; d) S. Nakamatsu, S. Toyota, W. Jones, F. Toda, *Chem. Commun.* **2005**, 3808.

[9] a) A. Grunenberg, J. O. Henck, H. W. Siesler, *Int. J. Pharm.* **1996**, *129*, 147; b) L. Yu, *J. Pharm. Sci.* **1995**, *84*, 966; c) M. Brandstaetter, H. Grimm, *Mikrochim. Acta* **1956**, *7–8*, 1175.

[10] M. R. Chierotti, R. Gobetto, *Chem. Commun.* **2008**, 1621.

[11] a) D. Braga, L. Maini, C. Fagnano, P. Taddei, M. R. Chierotti, R. Gobetto, *Chem. Eur. J.* **2007**, *13*, 1222; b) R. K. Harris, *J. Pharm. Pharmacol.* **2007**, *59*, 225; c) D. Braga, M. R. Chierotti, N. Garino, R. Gobetto, F. Grepioni, M. Polito, A. Viale, *Organometallics* **2007**, *26*, 2266.

[12] a) M. R. Chierotti, L. Garlaschelli, R. Gobetto, C. Nervi, G. Peli, A. Sironi, R. Della Pergola, *Eur. J. Inorg. Chem.* **2007**, *22*, 3477; b) I. Schnell, B. Langer, S. H. M. Söntjens, R. P. Sijbesma, M. H. P. van Genderen, H. W. Spiess, *Phys. Chem. Chem. Phys.* **2002**, *4*, 3750; c) R. K. Harris, *Solid State Sci.* **2004**, *6*, 1025.

[13] a) E. Diez-Pena, I. Quijada-Garrido, J. M. Barrales-Rienda, I. Schnell, H. W. Spiess, *Macromol. Chem. Phys.* **2004**, *205*, 430; b) D. Braga, F. Grepioni, M. Polito, M. R. Chierotti, S. Ellena, R. Gobetto, *Organometallics* **2006**, *25*, 4627; c) R. Gobetto, C. Nervi, M. R. Chierotti, D. Braga, L. Maini, F. Grepioni, R. K. Harris, P. Hodgkinson, *Chem. Eur. J.* **2005**, *11*, 7461.

[14] a) I. Schnell, S. P. Brown, H. Y. Low, H. Ishida, H. W. Spiess, *J. Am. Chem. Soc.* **1998**, *120*, 11784; b) S. P. Brown, I. Schnell, J. D. Brand, K. Mullen, H. W. Spiess, *J. Mol. Struct.* **2000**, *521*, 179.

[15] a) Z. Gu, A. McDermott, *J. Am. Chem. Soc.* **1993**, *115*, 4282; b) A. Naito, S. Ganapathy, K. Akasaka, C. J. McDowell, *J. Chem. Phys.* **1981**, *74*, 3198; c) D. Braga, L. Maini, G. de Sanctis, K. Rubini, F. Grepioni, M. R. Chierotti, R. Gobetto, *Chem. Eur. J.* **2003**, *9*, 5538; d) R. Gobetto, C. Nervi, E. Valfrè, M. R. Chierotti, D. Braga, L. Maini, F. Grepioni, R. K. Harris, P. Y. Ghi, *Chem. Mater.* **2005**, *17*, 1457; e) R. O. Duthaler, J. D. Roberts, *J. Magn. Reson.* **1979**, *34*, 129; f) R. E. Botto, J. D. Roberts, *J. Org. Chem.* **1977**, *42*, 2247.

[16] a) D. Braga, S. L. Giaffreda, F. Grepioni, M. R. Chierotti, R. Gobetto, G. Palladino, M. Polito, *CrystEngComm* **2007**, *9*, 879; b) I. G. Shenderovich, G. Buntkowsky, A. Schreiber, E. Gedat, S. Sharif, J. Albrecht, N. S. Golubev, G. H. Findenegg, H.-H. Limbach, *J. Phys. Chem. B* **2003**, *107*, 11924.

[17] I. Schnell, H. W. Spiess, *J. Magn. Reson.* **2001**, *151*, 153.

[18] a) C. B. Aakeröy, D. J. Salmon, *CrystEngComm* **2005**, *7*, 439; b) S. L. Childs, G. P. Stahly, A. Park, *Mol. Pharm.* **2007**, *4*, 323.

[19] a) G. M. Sheldrick, SHELX97, Program for Crystal Structure Determination, University of Göttingen, Göttingen, Germany, **1997**; b) E. Keller, SCHAKAL99, Graphical Representation of Molecular Models, University of Freiburg, Germany, **1999**; c) A. L. Spek, *Acta Crystallogr. Sect. A* **1990**, *46*, C31; d) PowderCell programmed by W. Kraus and G. Nolze (BAM Berlin), subgroups derived by U. Müller (Gh Kassel).

[20] a) M. Feike, D. E. Demco, R. Graf, J. Gottwald, S. Hafner, H. W. Spiess, *J. Magn. Reson. Ser. A* **1996**, *122*, 214; b) W. Sommer, J. Gottwald, D. E. Demco, H. W. Spiess, *J. Magn. Reson. Ser. A* **1995**, *113*, 131.

Received: May 30, 2008
Published online: September 18, 2008

